Proceedings of Symposium on Ultrasonic Electronics, Vol. 31 (2010) pp. 67-68
6-8 December, 2010

Evaluation of acoustic anisotropy to image defects in weld metal by ultrasonic phased array

超音波フェーズドアレイによる溶接金属中の欠陥映像化のための音響異方性の評価

Yohei Shintaku[1†], Yoshikazu Ohara[1] and Kazushi Yamanaka[1] ([1]Facult. Eng., Tohoku Univ.);
新宅　洋平[1‡]，小原　良和[1]，山中　一司[1] ([1]東北大 工)

1. Background

Ultrasonic Testing is an effective method for evaluation of cracks in structures. Recently, in particular, ultrasonic phased array (PA) has become promising. However, there is a problem of underestimation or overlook of stress corrosion cracks in weld metals in atomic power plants. One of the causes is the strong anisotropy of columnar crystals grown in weld metals. It is thus difficult to evaluate those cracks with high sensitivity and accuracy by conventional PA assuming isotropic material. However, analysis of anisotropy for a compensation of the shift of defect image in PA has not been performed.

In this study, we compare the results of experiment and theoretical simulation by the finite difference time domain (FDTD)[1)] method in measuring a slit inside a Ni-base weld metal of Inconel 600. And then, we evaluate an anisotropy of weld metal and the shift of defect image in PA.

2. Principle of simulation

Propagation of elastic waves is governed by Newton's second law and Hook's law. They are described as

$$\rho \frac{\partial^2 \mathbf{U}}{\partial t^2} = \nabla_T \mathbf{T} \quad (1) \ , \ \mathbf{T} = [c] \nabla_S \mathbf{U} \quad (2),$$

where **U** is displacement vector, **T** is stress tensor, $[c]$ is elastic stiffness tensor and ∇_T, ∇_S are spatial differential operators[2]. In FDTD method, the points for computation of particle velocity and stress are aligned on a spatial grid as shown in **Fig.1(a)**. In 2D problem of cubic crystals (under assumption that all components are uniform in y direction and u_y=0), difference in time of $\dot{w}$ (particle velocity in z direction) is obtained from

$$\left[\dot{w}(t+\Delta t) - \dot{w}(t)\right]\rho / \Delta t \qquad (3)$$
$$= \left[\tau_{zz}(z+\Delta z) - \tau_{zz}(z)\right]/\Delta z + \left[\tau_{xz}(x+\Delta x) - \tau_{xz}(x)\right]/\Delta x$$

where ρ is density and τ_{zz} and τ_{xz} are tensile stress and shear stress in z direction. Similarly, $\dot{u}$ (particle velocity in x direction) is obtained. Differences in time of τ_{zz} and τ_{xz} are obtained from

$$\left[\tau_{zz}(t+\Delta t) - \tau_{zz}(t)\right]/\Delta t \qquad (4)$$
$$= \left[\dot{w}(z+\Delta z) - \dot{w}(z)\right]c_{11}/\Delta z + \left[\dot{u}(x+\Delta x) - \dot{u}(x)\right]c_{12}/\Delta x,$$
$$\left[\tau_{xz}(t+\Delta t) - \tau_{xz}(t)\right]/\Delta t \qquad (5)$$
$$= c_{44}\left(\left[\dot{u}(z+\Delta z) - \dot{u}(z)\right]/\Delta z + \left[\dot{w}(x+\Delta x) - \dot{w}(x)\right]/\Delta x\right)$$

where c_{11}, c_{12} and c_{44} are elastic constants. Now as a boundary condition on the top and bottom surfaces of a specimen and a slit (**Fig1.(b)** was used in this study), all stresses are zero and ρ for computation of $\dot{w}$ and $\dot{u}$ are replaced by ρ/4 and 3ρ/4 respectively.[1)] Also we introduce anisotropic factor[2)] $\eta = 2c_{44}/(c_{11}-c_{12})$ and compute **Eqs.(4) (5)** with it and c_{44N} obtained by normalizing c_{44} with c_{11}.

As a initial condition, we give

$$\dot{w}_{in}(x,t) = A_s(x)A_t(t)\sin(2\pi f t) \qquad (6)$$

on top surface of specimen over a range covered with an array sensor within a duration time T_C=N_C/f, where f is frequency, N_C is a number of cycles,

$$A_s(x) = \exp\left(-\frac{(x-x_o)^2}{x_W}\right) \qquad (7)$$

where x_o is a central position of the array sensor and x_W expresses a width of Gaussian distribution and

$$A_t(t) = \begin{cases} 1/2\left[1-\cos(5\pi t/T_C)\right] & (t < T_C/5) \\ 1 & (T_C/5 \le t < 4T_C/5) \\ 1/2\left[1+\cos(5\pi(t-4T_C/5)/T_C)\right] & (4T_C/5 \le t). \end{cases} \qquad (8)$$

We output the value of $\dot{w}$ at positions of each element of the array sensor as received waveforms. Finally, we form an image by shift and summation of waveforms following general PA algorithm.

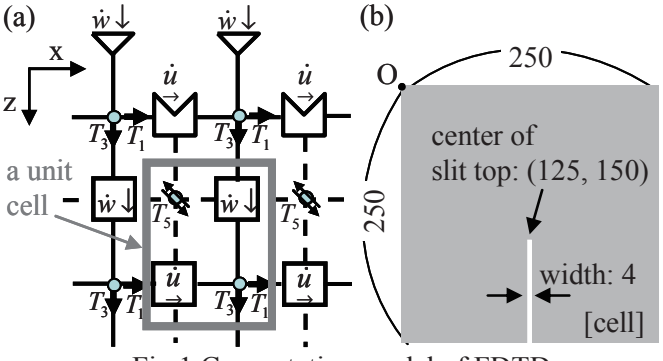

Fig.1 Computation model of FDTD.

3. Fabrication of the specimen and experiment

We welded stainless steel (SUS316L) with Inconel 600 as a weld metal, and then a slit was introduced along the welding line. The thickness of the specimen was 25 mm.

In the experiment, we evaluate the slit by PA with an array sensor (5 MHz, 16 elements, 0.5 mm pitch) located as shown in **Fig.2(a)**. The PA image is shown in **(b)**, where three responses are formed by input (1), scattering at the slit tip (2) and scattering at the back surface (3), respectively. As a result, the slit tip was imaged with a lateral shift of 3.5 mm from the true position.

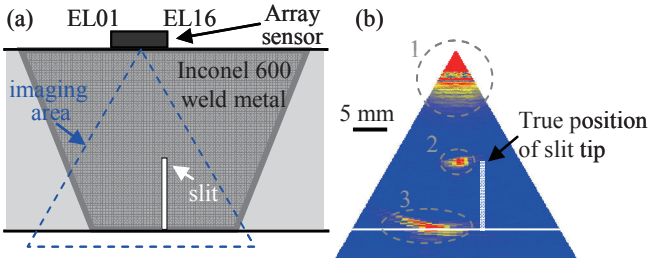

Fig.2 Imaging of a slit in weld metal:
(a) experimental condition, (b) PA image.

4. Simulation and comparison with experiment

First we simulated a PA image of a slit in isotropic material with η=1.0 and c_{44N}=0.42. The size of a slit and the location and design of an array sensor followed experimental condition in **Sec.3**. The parameters of incident wave was f=5 MHz and N_C=2, and we applied a delay law for focusing to the slit tip. The simulated $\dot{w}$ distributions are shown in **Fig.3(a)(b)**. The focusing of ultrasound to the slit tip and the scattering in a circle were observed respectively. Received waveforms at each element of the array sensor are shown in **(c)**, and you can observe the echoes from the slit tip and the back surface clearly. The PA image is shown in **(d)**. As a result, the slit tip imaged with no shift.

Next, we simulated with η=1.58 to assume anisotropy of the weld metal. The other conditions had no difference with ones of above simulation. In **Fig.4(a),** focusing to the slit tip was not performed well and the deflection angle was larger than that in **Fig.3(a)**. **In Fig.4(b)**, the scattered wave appeared as a distorted circle. The amplitude of the echoes in **Fig.4(c)** was smaller than that in **Fig.3(c)**. The PA image is shown in **Fig.4(d)**. The slit tip was imaged with a lateral shift of 1.4 mm from the true position.

5. Conclusion

Based on exact calculation of anisotropic propagation of elastic wave and phased array algorithm, we succeeded in reproducing the shift of defect image. This result is useful to reduce errors in testing Ni-base alloy welds in atomic power plants. It will significantly contribute to enhance our safety. As a next step, we introduce a closed-crack model in FDTD and evaluate the nonlinear response at closed cracks.[3)]

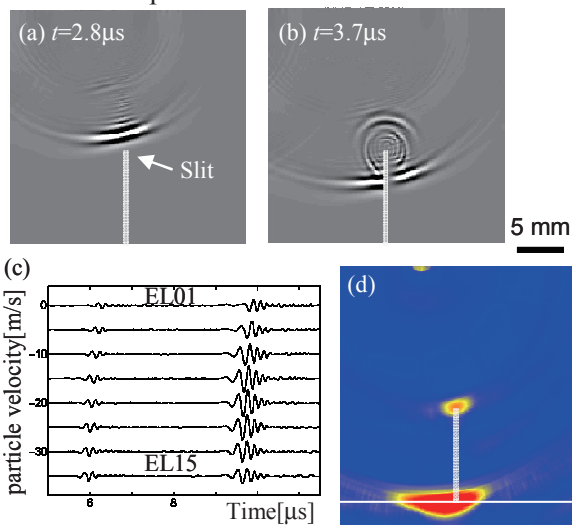

Fig.3 Result of FDTD assuming an isotropic material:(a)(b) $\dot{w}$ distributions, (c) received waveform and (d) PA image.

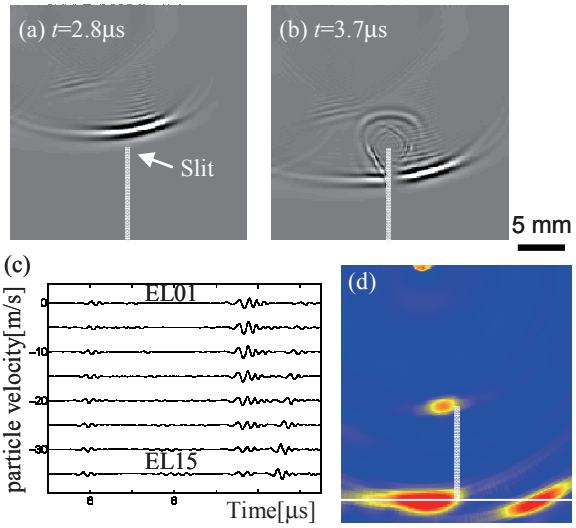

Fig.4 Result of FDTD assuming an anisotropy.

Acknowledgment

This work was supported by Project of Nuclear and Industrial Safety Agency, METI, and Grants-in-Aid for Science Research (Nos. 21686069 and 21246105) in Japan.

References

1. Masahiro Sato: *FDTD* (*Basic analysis of elastic vibrations and waves by FDTD method*) (Morikita, Tokyo, 2003) [in Japanese].
2. B.A.Auld: "*Acoustic Fields and Waves in Solids Volume I*" (John Wiley & Sons Inc, 1973).
3. K. Yamanaka, T. Mihara, T. Tsuji: Jpn. J. Appl. Phys. **43** (2004) 3082.